JACS
JOURNAL OF THE AMERICAN CHEMICAL SOCIETY
Communication
pubs.acs.org/JACS

A Robust Probe for Lighting Up Intracellular Telomerase via Primer Extension To Open a Nicked Molecular Beacon

Ruocan Qian,[†] Lin Ding,[†] Liwen Yan, Manfei Lin, and Huangxian Ju*

State Key Laboratory of Analytical Chemistry for Life Science, School of Chemistry and Chemical Engineering, Nanjing University, Nanjing 210093, P. R. China

Supporting Information

ABSTRACT: A nicked molecular beacon (MB)-functionalized probe has been designed for in situ imaging and detection of intracellular telomerase activity. The nick separates the MB into two segments: a shorter telomerase primer (TSP) sequence as a part of the 5′-end stem and a longer sequence to form a loop with one thiol-labeled 3′-end stem. The MB can be opened by substitutional hybridization of the telomerase-triggered stem elongation product, which leads to separation of the Cy5 at the 5′-end nick from the gold nanoparticle (AuNP) as the nanocarrier and thus inhibits the energy transfer from Cy5 to AuNP. Upon endocytosis of the probe, the TSP can be extended by intracellular telomerase at its 3′ end to produce the telomeric repeated sequence, which leads to the inner chain substitution and thus turns on the fluorescence of Cy5. The probe provides a one-step incubation technique for quantification and monitoring of the telomerase activity in living cells. The practicality of the proposed approach for distinguishing tumor cells from normal cells and monitoring the decrease of telomerase activity during treatment with antitumor drugs demonstrates its potential in clinical diagnostic and therapeutic monitoring.

Human telomerase is a ribonucleoprotein that can add hexamer DNA sequence repeats to the end of telomeres through its RNA template.[1] In normal cells, telomeres are shortened after each replication cycle, which leads to cell senescence and death.[2−4] In contrast, in most types of cancer cells, the length of telomeres is maintained because of the upregulation or activation of telomerase, which makes cancer cells divide indefinitely.[5−7] High expression of telomerase activity has also been detected in metastatic cancer tissues.[1] Therefore, telomerase has been regarded as a promising tumor marker, and its detection is of great meaning to cancer diagnosis, therapy, and monitoring.[8−13]

Since the discovery of telomerase in 1985,[14] a variety of strategies have been proposed for the detection of telomerase activity. These strategies can be divided into three main categories: polymerase chain reaction (PCR)-based classic telomeric repeat amplification protocols (TRAPs),[15−17] isothermal DNA amplification[18−20] or DNAzyme-based methods,[21,22] and nanomaterial-based biosensing protocols.[23−25] Although these methods have achieved satisfactory sensitivity and limits of detection, most of them are incompetent to provide telomerase information in complex biological environments, particularly in living cells, because these methods generally use cell lysates as the samples.

Focusing on this limitation, our previous work designed a telomerase-regulated release of fluorescein from a mesoporous silica nanoprobe (MSN) to develop a noninvasive method for in situ detection of intracellular telomerase.[26] However, the probe preparation was complicated, and the probe displayed a certain degree of nonspecific release. More importantly, the response process involved multiple stages, thus increasing the environmental susceptibility of the probe. Therefore, the development of robust methods for in situ tracking of intracellular telomerase activity is still of great significance.

Inspired by the DNA nature of telomerase primer and its extension product as well as the advantages of gold nanoparticles (AuNPs) as the substrate for immobilization[27−31] and protection[32,33] of DNA and the quencher of fluorescent dyes via fluorescence resonance energy transfer (FRET),[34] in this work we have designed a nicked molecular beacon (MB)-functionalized probe. The nicked MB can be opened by substitutional hybridization of the telomerase-triggered stem elongation product to produce a telomerase-activity-related fluorescence signal. Thus, this probe can be conveniently used for in situ imaging and detection of intracellular telomerase activity through a one-step incubation procedure (Scheme 1).

The designed MB contains a nick on the 5′-end stem that separates the MB into two segments: a shorter telomerase primer (TSP) sequence as a part of the 5′-end stem and a longer sequence (l-MB) to form a loop with a thiol-labeled 3′-end stem. After conjugation of the 3′ end to the AuNP, the fluorescence of the Cy5 label at the 5′ end of l-MB can be quenched via FRET.[34] In the presence of telomerase in the cellular environment, the TSP can be elongated from its 3′ end to produce a telomeric repeated sequence that is just complementary to the corresponding stem at the 3′ end of l-MB, which leads to substitutional hybridization to open the hairpin. This process turns on the fluorescence switch as a result of the departure of Cy5 from the AuNP surface, thus lighting up the telomerase. The telomerase-triggered switch integrates its recognition and enzymatic amplification functions and thus possesses good specificity and high sensitivity.

AuNPs were synthesized by a reported aqueous-phase method.[35] The probe was prepared by incubating a mixture of TSP, l-MB, and AuNPs. Transmission electron microscopy (TEM) of the AuNPs showed an average diameter of 13 nm

Received: April 30, 2014
Published: May 23, 2014

dx.doi.org/10.1021/ja5042995 | J. Am. Chem. Soc. 2014, 136, 8205−8208

Scheme 1. Schematic Illustration of the Nicked Molecular Beacon-Functionalized Gold Nanoparticle (Probe) for in Situ Analysis of Intracellular Telomerase

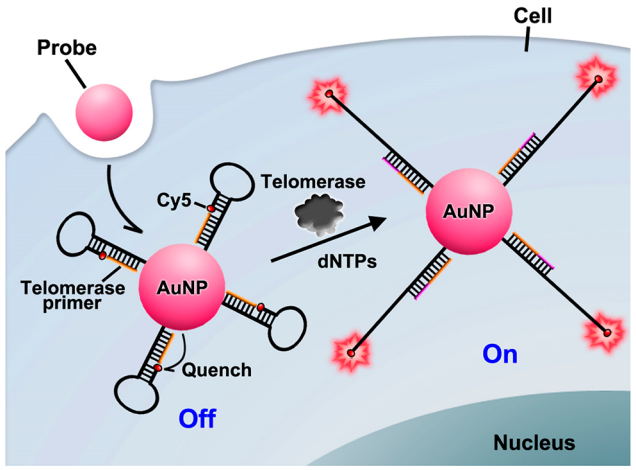

with a narrow distribution (Figure 1a), which was consistent with the dynamic light scattering (DLS) result of 14.3 nm (Figure 1b). After the AuNPs were functionalized with the nicked MBs, the UV–vis spectrum showed the characteristic peak of DNA at 260 nm (Figure 1c) and the obtained probe showed a more negative charge compared with the AuNPs

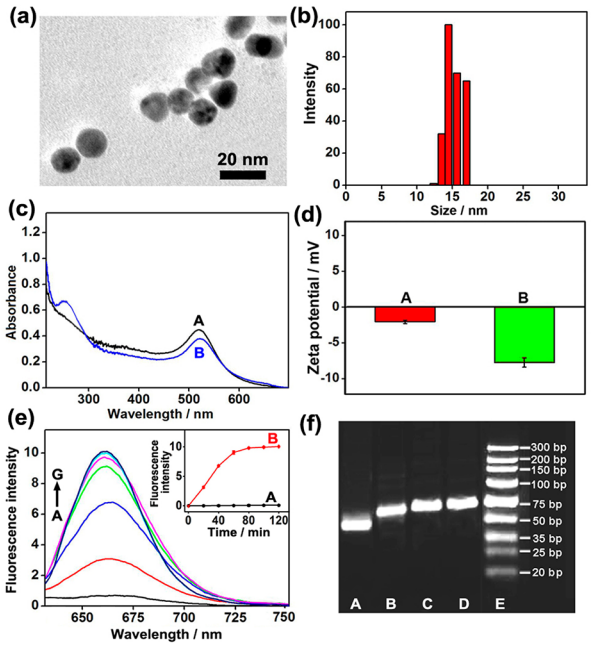

Figure 1. (a) TEM image of AuNPs. (b) DLS characterization of the prepared AuNPs. (c) UV–vis spectra of (A) AuNPs and (B) the probe. (d) Zeta potentials of (A) AuNPs and (B) the probe in H_2O. (e) Fluorescence spectra of the probe after incubation with dNTPs (100 μM each) and 0.4 IU L^{-1} telomerase for 0, 20, 40, 60, 80, 100, and 120 min (from A to G). Inset in (e): Plots of fluorescence intensity vs incubation time of the probe with dNTPs in (A) the absence and (B) the presence of 0.4 IU L^{-1} telomerase. (f) Electrophoresis image of (A) l-MB; (B) the mixture of TSP and l-MB after incubation for 1 h; (C) the mixture of nicked MBs, dNTPs, and cell extract after incubation for 1 h; (D) the mixture of nicked MBs, dNTPs, and telomerase after incubation for 1 h; and (E) ladder DNA.

(Figure 1d), confirming the successful binding of the nicked MBs to AuNPs. The number of MBs assembled on each probe was determined to be around 90 [Figure S1 in the Supporting Information (SI)].[36]

In order to test the response of the probe to telomerase, the fluorescence intensity of the mixture of the probe, dNTPs, and telomerase in phosphate-buffered saline (PBS) was recorded at different incubation times (Figure 1e). At the beginning, almost no fluorescence was detected at the excitation wavelength of 600 nm for Cy5, suggesting that the Cy5 fluorescence was quenched by the AuNPs. The fluorescence intensity gradually increased with the increasing incubation time and tended to a constant value after 60 min (Figure 1e inset, curve B), indicating the switch feature of the probe due to opening of the MBs. Importantly, no change in the fluorescence intensity was observed in the absence of telomerase (Figure 1e inset, curve A), verifying the good stability of the probe and the telomerase-triggered fluorescence switch. The stability of the probe was much better than that of the previously reported fluorescein-sealed MSN,[26] which showed slow leakage of fluorescein in the absence of telomerase. Furthermore, the "off/on" signal switch displayed similar changes in complex media such as DMEM and RPMI 1640 (Figure S2a–c), while the fluorescence recovery efficiency was very low in deionized water (Figure S2d), indicating the dependence of probe response on salt. The probe also exhibited stable dispersion during the incubation process (Figure S2e).

The mechanism of switching via telomerase-triggered TSP elongation could be verified with gel electrophoresis. After incubation of TSP and l-MB for 1 h, the product was around 70 bp (Figure 1f, lane B), which was about 20 bp longer than l-MB (Figure 1f, lane A), confirming the formation of the nicked MB. After the nicked MB was mixed with dNTPs and cell extract or telomerase solution and incubated for 1 h, the lanes displayed a band at around 75 bp (Figure 1f, lanes C and D), which was about 6 bp longer than the nicked MB, demonstrating the extension of the inner TSP in the nicked MB by telomerase.

The extension of TSP led to the substitutional hybridization to open the hairpin. Thus, the concentration of the opened MB, [P], could be obtained from the fluorescence intensity shown in Figure 1e. From the plot of [P] versus reaction time (Figure S3a), the reaction rate (V) could be obtained at different times and was found to be proportional to the concentration of nicked MB (Figure S3b). This result indicated that the telomerase-triggered fluorescence recovery reaction was a pseudo-first-order reaction, and the rate constant was determined to be 0.026 min^{-1}.

The feasibility of the proposed probe for telomerase analysis was first investigated in the extract of HeLa cells by a standard addition method (see the SI). From the fluorescence spectra (Figure S4), the average telomerase activity in the extract of a single HeLa cell was calculated to be 3.1×10^{-11} IU, which is consistent with the result of our previous work (3.0×10^{-11} IU),[26] confirming the ability of the probe to quantify telomerase activity in a complex cell extract.

Prior to intracellular usage, the ability of AuNPs to protect the nicked MBs against enzymatic cleavage in an acidic environment was tested using DNase I as the model. Compared with telomerase-triggered fluorescence recovery, the mixture of probe and 2 μg of DNase I in pH 6 PBS showed negligible fluorescence after incubation for 2 h (Figure S5), indicating excellent protection ability against nuclease cleavage.[32,33]

dx.doi.org/10.1021/ja5042995 | J. Am. Chem. Soc. 2014, 136, 8205–8208

For in situ tracking of the intracellular telomerase activity with the probe, HeLa cells (0.5 mL, 1×10^6 mL^{-1}) were seeded in a 20 mm confocal dish for 24 h. After the addition of 25 μL of probe into the dish, it was sent for confocal observation. Within the initial 30 min, no obvious fluorescence signal could be observed. After 50 min, fluorescence emission occurred in the cytoplasm as a result of the opening of the nicked MBs, and its intensity gradually increased with increasing incubation time for telomerase-triggered TSP extension until it reached a maximum at 90 min (Figure 2a). The recovery of the fluorescence of Cy5 indicated the presence of telomerase in the cytoplasm near the nucleus.[37] A TEM image also confirmed the internalization and localization of the probe (Figure S6).

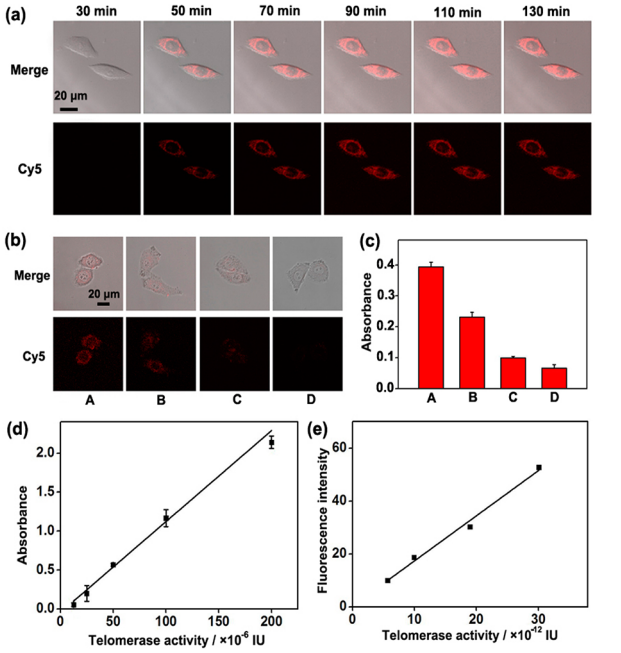

Figure 2. (a) Time course of confocal images of HeLa cells incubated with 25 μL of probe. (b) Confocal images of HeLa cells treated with 0, 60, 120, and 250 μg mL^{-1} EGCG (from A to D) and then incubated with 25 μL of probe for 1.5 h. (c) Absorbance of telomerase ELISA kit for cell extracts collected from HeLa cells treated with 0, 60, 120, and 250 μg mL^{-1} EGCG (from A to D). (d) Standard curve for in vitro detection of telomerase activity in solution with the ELISA kit. (e) Calibration curve for in vivo detection of intracellular telomerase activity in a single cell with the nicked-MB-functionalized probe.

The amount of probe used for in vivo detection of intracellular telomerase activity was optimized to be 25 μL by flow cytometry (Figure S7). The cytotoxicity of the probe was examined by MTT assay. The HeLa cells maintained about 90.7% of the cell viability after incubation with the probe for 3 h (Figure S8), indicating satisfactory low cytotoxicity. To demonstrate the specific opening of the nicked MBs triggered by telomerase in living cells, l-MB-functionalized AuNPs without the inner TSP were prepared and used in the same intracellular test. After 90 min of incubation, the cells showed negligible fluorescence (Figure S9), confirming the specific recognition and opening of the nicked MBs by telomerase-triggered TSP extension.

The low-cytotoxicity probe was first applied for dynamic monitoring of the variation of intracellular telomerase activity under the treatment of a model telomerase-inhibiting drug, epigallocatechin gallate (EGCG). After incubation of HeLa cells (0.5 mL, 1×10^6 mL^{-1}) with different amounts of EGCG in culture medium for 48 h, 25 μL of probe was added to each dish, and the mixtures were incubated for 1.5 h to perform the confocal imaging. As the amount of EGCG increased, the fluorescence intensity of the EGCG-treated cells became weaker (Figure 2b), indicating the dose-dependent inhibition of intracellular telomerase activity by EGCG. These results demonstrated that the probe can be used for noninvasive monitoring of intracellular telomerase activity, providing a potential tool for the screening of telomerase-related drugs.

The proposed probe could be used to quantify the intracellular telomerase activity. To obtain the calibration curve, model HeLa cells were first treated with different doses of EGCG for 48 h. After the EGCG-treated cells were incubated with 25 μL of probe, confocal images were taken to obtain the fluorescence intensity in the cell area (FI) (Figure 2b) with Adobe Photoshop software. The corresponding telomerase activities in single cells were then detected via in vitro enzyme-linked immunosorbent assay (ELISA) kit analysis of the cell extracts (Figure 2c) using a standard curve (Figure 2d). The calibration curve showed a linear relationship between the FI value and the intracellular telomerase activity (Figure 2e). The telomerase activity in a single HeLa cell was estimated to be 3.2×10^{-11} IU, in good agreement with the in vitro detection result of 3.1×10^{-11} IU using the cell extract and the value of 3.0×10^{-11} IU reported previously.[26]

The feasibility of the probe for in situ quantification of telomerase activity was further verified using various types of cells, such as MCF (breast cancer), BGC-823 (gastric cancer), BEL-7402 (liver cancer), and QSG-7701 (normal liver) cells. Confocal microscopy detection indicated that cancer cells showed higher telomerase activities than normal cells (Figure 3a). The telomerase activities in single HeLa, MCF, BGC, BEL, and QSG cells were estimated to be 3.1×10^{-11}, 1.4×10^{-11}, 2.5×10^{-11}, 2.1×10^{-11}, and 8.4×10^{-13} IU, respectively (Figure 3b). The distinct activities of tumor and normal cells were consistent with the results obtained using flow cytometry detection (Figure S10). Inductively coupled plasma atomic emission spectroscopy (ICP-AES) was used to analyze the cellular uptake of the probe.[38] Different types of cells as well as EGCG-treated HeLa cells showed similar uptake amounts of probe after they were incubated with the probe (Figure S11), excluding the contribution of the difference in probe uptake to the fluorescence signal. Thus, the proposed strategy possesses broad applicability for monitoring changes in intracellular telomerase activity and distinguishing different cells, particularly cancer cells from normal cells.

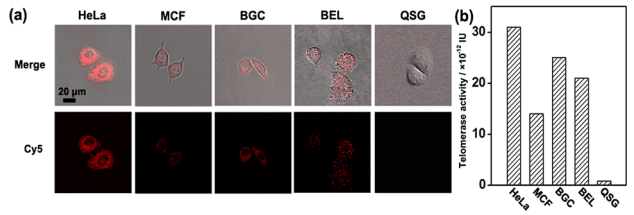

Figure 3. (a) Confocal images of HeLa, MCF, BGC, BEL, and QSG cells (0.5 mL, 1×10^6 mL^{-1}) after incubation with 25 μL of probe for 1.5 h. (b) Telomerase activities in single cells.

In conclusion, in this work we have designed a nicked MB for the construction of a novel functionalized probe for in situ detection of intracellular telomerase activity. This probe

dx.doi.org/10.1021/ja5042995 | J. Am. Chem. Soc. 2014, 136, 8205−8208

possesses synthetic convenience, intracellular stability, cytocompatibility, and good specificity for recognition of telomerase. The telomerase-triggered TSP elongation of the MBs leads to the inner chain substitution hybridization, which opens the hairpin and lights up the telomerase. The fluorescence switch can be achieved in cytoplasm through one-step incubation of the living cells with the probe. The practicality of the proposed probe has been demonstrated by dynamic monitoring of the dose-dependent change of telomerase activity in response to a telomerase-related drug, in situ quantification of the intracellular telomerase activity, and distinguishing of different tumor cells from each other and from normal cells. We anticipate that this probe will accelerate the uncovering of the basic role of telomerase in various biological events and contribute to clinical diagnosis and therapeutic monitoring of cancer.

■ ASSOCIATED CONTENT

Ⓢ Supporting Information

Experimental details and figures. This material is available free of charge via the Internet at http://pubs.acs.org.

■ AUTHOR INFORMATION

Corresponding Author

hxju@nju.edu.cn

Author Contributions

†R.Q. and L.D. contributed equally.

Notes

The authors declare no competing financial interest.

■ ACKNOWLEDGMENTS

This work was financially supported by the National Basic Research Program (2010CB732400, 2014CB744501) and the National Natural Science Foundation of China (21322506, 21135002, 21121091, 91213301).

■ REFERENCES

(1) Harley, C. B. *Nat. Rev. Cancer* **2008**, *8*, 167.
(2) Blasco, M. A. *Nat. Rev. Genet.* **2005**, *6*, 611.
(3) Rodier, F.; Campisi, J. *J. Cell Biol.* **2011**, *192*, 547.
(4) Shay, J. W.; Wright, W. E. *Carcinogenesis* **2005**, *26*, 867.
(5) Petel, S. D.; Isalan, M.; Gavory, G.; Ladame, S.; Choo, Y.; Balasubramanian, S. *Biochemistry* **2004**, *43*, 13452.
(6) Shay, J. W.; Bacchetti, S. *J. Cancer* **1997**, *33*, 787.
(7) Masutomi, K.; Yu, E. Y.; Khurts, S. *Cell* **2003**, *114*, 241.
(8) Lu, L. G.; Zhang, C.; Zhu, G. J.; Irwin, M.; Risch, H.; Menato, G.; Mitidieri, M.; Katsaros, D.; Yu, H. *Breast Cancer Res.* **2011**, *13*, R56.
(9) Mergny, J. L.; Riou, J. F.; Mailliet, P.; Teulade-Fichou, M. P.; Gilson, E. *Nucleic Acids Res.* **2002**, *30*, 839.
(10) Zhou, X. M.; Xing, D. *Chem. Soc. Rev.* **2012**, *41*, 4643.
(11) Shay, J. W.; Zou, Y.; Hlyama, E.; Wright, W. E. *Hum. Mol. Genet.* **2011**, *10*, 677.
(12) Williams, S. C. P. *Nat. Med.* **2013**, *19*, 6.
(13) Agrawal, A.; Dang, S.; Gabrani, R. *Recent Pat. Anti-Cancer Drug Discovery* **2012**, *7*, 102.
(14) Greider, C. W.; Blackburn, E. H. *Cell* **1985**, *43*, 405.
(15) Herbert, B. S.; Hochreiter, A. E.; Wright, W. E.; Shay, J. W. *Nat. Protoc.* **2006**, *1*, 1583.
(16) Kim, N. W.; Wu, F. *Nucleic Acids Res.* **1997**, *25*, 2595.
(17) Hou, M.; Xu, D. W.; Bjorkholm, M.; Gruber, A. *Clin. Chem.* **2001**, *47*, 519.
(18) Tian, L. L.; Weizmann, Y. *J. Am. Chem. Soc.* **2013**, *135*, 1661.
(19) Wang, L. J.; Zhang, Y.; Zhang, C. Y. *Anal. Chem.* **2013**, *85*, 11509.
(20) Zhao, Y. X.; Qi, L.; Chen, F.; Zhao, Y.; Fan, C. H. *Biosens. Bioelectron.* **2013**, *41*, 764.
(21) Wang, H.; Donovan, J.; Meng, L.; Zhao, Z. L.; Kim, Y.; Ye, M.; Tan, W. H. *Chem.—Eur. J.* **2013**, *19*, 4633.
(22) Xiao, Y.; Pavlov, V.; Niazov, T.; Dishon, A.; Kotler, M.; Willher, I. *J. Am. Chem. Soc.* **2004**, *126*, 7430.
(23) Patolsky, F.; Gill, R.; Weizmann, Y.; Mokari, T.; Banin, U.; Willner, I. *J. Am. Chem. Soc.* **2003**, *125*, 13918.
(24) Li, Y.; Li, X.; Ji, X. T.; Lia, X. M. *Biosens. Bioelectron.* **2011**, *26*, 4095.
(25) Wang, J. S.; Wu, L.; Ren, J. S.; Qu, X. G. *Small* **2012**, *8*, 259.
(26) Qian, R. C.; Ding, L.; Ju, H. X. *J. Am. Chem. Soc.* **2013**, *135*, 13282.
(27) Duncan, B.; Kim, C.; Rotello, V. M. *J. Controlled Release* **2010**, *148*, 122.
(28) Li, F.; Zhang, H. Q.; Dever, B.; Li, X. F.; Le, X. C. *Bioconjugate Chem.* **2013**, *24*, 1790.
(29) Boisselier, E.; Astruc, D. *Chem. Soc. Rev.* **2009**, *38*, 1759.
(30) Guo, L. H.; Xu, Y.; Ferhan, A. R.; Chen, G. N.; Kim, D. H. *J. Am. Chem. Soc.* **2013**, *135*, 12338.
(31) Wu, P. W.; Hwang, K.; Lan, T.; Lu, Y. *J. Am. Chem. Soc.* **2013**, *135*, 5254.
(32) Giljohann, D. A.; Seferos, D. S.; Patel, P. C.; Millstone, J. E.; Rosi, N. L.; Mirkin, C. A. *Nano Lett.* **2007**, *7*, 3818.
(33) Seferos, D. S.; Giljohann, D. A.; Hill, H. D.; Prigodich, A. E.; Mirkin, C. A. *J. Am. Chem. Soc.* **2007**, *129*, 15477.
(34) Yun, C. S.; Javier, A.; Jennings, T.; Fisher, M.; Hira, S.; Peterson, S.; Hopkins, B.; Reich, N. O.; Strouse, G. F. *J. Am. Chem. Soc.* **2005**, *127*, 3115.
(35) Grabar, K. C.; Freeman, R. G.; Hommer, M. B.; Natan, M. J. *Anal. Chem.* **1995**, *67*, 735.
(36) Burda, C.; Chen, X. B.; Narayanan, R.; El-Sayed, M. A. *Chem. Rev.* **2005**, *105*, 1025.
(37) Morin, G. B. *Cell* **1989**, *59*, 521.
(38) Chithrani, B. D.; Ghazani, A. A.; Chan, W. C. W. *Nano Lett.* **2006**, *6*, 662.